

Micro magnetofluidics – interactions between magnetism and fluid flow on the microscale

Nam-Trung Nguyen

Received: date / Accepted: date

Abstract Micro magnetofluidics refers to the science and technology that combines magnetism with microfluidics to gain new functionalities. Magnetism has been used for actuation, manipulation and detection in microfluidics. In turn, microfluidic phenomena can be used for making tunable magnetic devices. This paper presents a systematic review on the interactions between magnetism and fluid flow on the microscale. The review rather focuses on physical and engineering aspects of micro magnetofluidics, than on the biological applications which have been addressed in a number of previous excellent reviews. The field of micro magnetofluidics can be categorized according to the type of the working fluids and the associated microscale phenomena of established research fields such as magnetohydrodynamics (MHD), ferrohydrodynamics (FHD), magnetorheology (MR) and magnetophoresis (MP). Furthermore, similar to microfluidics the field can also be categorized as continuous and digital micro magnetofluidics. Starting with the analysis of possible magnetic forces in microscale and the impact of miniaturization on these forces, the paper revisits the use of magnetism for controlling fluidic functions such as pumping, mixing, magnetowetting as well as magnetic manipulation of particles. Based on the observations made with the state of the art of the field micro magnetofluidics, the paper presents some perspectives on the possible future development of this field. While the use of magnetism in microfluidics is relatively established, possible new

phenomena and applications can be explored by utilizing flow of magnetic and electrically conducting fluids.

Keywords Micro magnetofluidics · Magnetism · Microfluidics · Magnetic bead · Ferro fluid

1 Introduction

Magnetofluidics traditionally refers to a class of devices that utilize a magnetic fluid for sensing and actuating functions. These devices were used as sensor for applications such as hearing aid and accelerometer. However, the term of “magnetofluidics” is used here for the broader research field involving magnetism and fluid flows. Figure 1 shows the basic relationships between the four principal fields of physics with the most applications: fluidics, electrics, optics, and magnetism. The links between these fields cover most modern technologies, especially micro/nanotechnologies. However, efforts on the exploration of magnetofluidics in microscale and its applications have been scattered. Many possibly interesting phenomena have been neglected due to the lack of a systematic approach. Compared to an electric field, a magnetic field has various advantages in microfluidic applications. Magnetic manipulation can utilize external magnets that are not in direct contact with the fluid. Nonmagnetic molecules and cells can be attached to magnetic beads, so that they can be sorted and detected by an external magnetic field. In contrast to electric concepts, magnetic manipulation and detection are not affected by other parameters such as surface charges, pH and ion concentration. In most cases, magnetic manipulation does not induce heating and does not require expensive external systems as compared to optical concepts.

Nam-Trung Nguyen
School of Mechanical and Aerospace Engineering, Nanyang Technological University, 50 Nanyang Avenue, Singapore 639798
Tel.: +65-6790 4457
Fax: +65-6792 4062
E-mail: mntnguyen@ntu.edu.sg

A number of excellent reviews on applications of magnetism in microfluidics exist in the literature. However, the scopes of these reviews are limited to phenomena with existing biological applications. Gijs reviewed the use of magnetic beads for analytical applications [28]. Later, Gijs and colleagues followed up with a more comprehensive and updated review on applications of magnetic particles for biological analysis and catalysis [29]. Pamme extended the scope in her review and covered a wider range of applications of magnetism in microfluidics: pumping, mixing, manipulation of particles and magnetic detection [63]. Pamme's review was the first attempt to look at the field from a broader perspective and to consider both ways of the interactions between magnetism and microfluidics. Since Pamme's review was only based on reported works, many potentially interesting phenomena were neglected. Weston et al. discussed the use of different types of magnetic forces for fluid motion [88]. Weston's review was based on the discussion of possible magnetic forces followed by their applications. Fisher and Ghosh reviewed the use of magnetism for propulsion of swimming particles [23]. This minireview offers a new perspective on "smart" magnetic particles. Magnetic micro and nanostructures with unique shapes other than the conventional sphere can be controlled with an external magnetic field. Weddemann et al. reviewed the implementation of magnetic components in total analysis systems for biomedical applications [86]. The scope of this review was limited to the detection and manipulation of magnetic beads. Similarly, the review of Suwa and Watarai only focuses on the manipulation and detection of microparticles [79]. Ganguly and Puri reviewed microfluidic transport of ferrofluid and magnetic particles in MEMS, Bio-MEMS devices [25]. Friedman and Yellen discussed the physical fundamentals of magnetic separation, manipulation and assembly using relatively simple but useful scaling analysis of the magnetic force and its counter parts [24].

In this paper, micro magnetofluidics (MMF) is understood as the science and technology that combines magnetism with microfluidics to gain new functionalities. The present review rather focuses on physical and engineering aspects of micro magnetofluidics, than on the biological applications which have been addressed in the above mentioned excellent reviews. The field of micro magnetofluidics can be categorized according to the type of the working fluids, and the microscale phenomena of established research fields such as *magnetohydrodynamics* (MHD), *ferrohydrodynamics* (FHD), *magnetorheology* (MR) and *magnetophoresis* (MP). Furthermore, the field can also be categorized as continuous and digital micro magnetofluidics as in traditional mi-

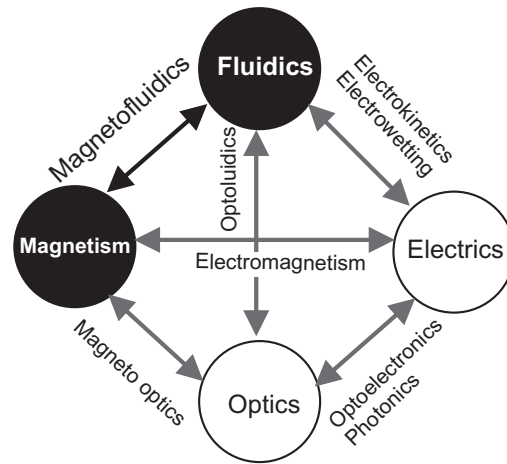


Fig. 1 The basic domains of physics and their interfaces.

crofluidics. Figure 2 shows an overview of micro magnetofluidics and its subfields. In general, the field can be categorized according to the properties of the fluids or to the ways the fluids are handled. The majority of magnetofluidic phenomena are based on electrically conducting fluids and magnetic fluids. The mutual interaction of magnetic field and the flow of electrically conducting fluids is covered by MHD, which is well established and studied in the past hundred years [17]. The fluids need to be electrically conducting and non-magnetic, thus are limited to liquid metals, plasmas and strong electrolytes. The traditional applications of MHD are geophysics, astrophysics, plasmaphysic and metallurgy.

Magnetic fluid consists of a carrier fluid and a suspension of magnetic particles. Depending on the size of the magnetic particles, the magnetic fluid behaves differently leading to three main areas of FHD, MR and MP. If the magnetic particles are smaller than about 10 nm, the thermal energy dominates over the magnetic energy induced by an external magnetic field. Thus, the particles can disperse well in the carrier fluid. The whole fluid behaves as a paramagnetic liquid and is called ferrofluid. If the magnetic particles is large enough, ranging from 10 nm to 10 μm , they interact and react to the external magnetic field changing the viscosity of the fluid. The fluid is then called magnetorheological fluid. For magnetic particles on the order of several microns or larger, the magnetic particles need to be considered individually as discrete entities, leading to the field of magnetophoresis.

According to the properties of the fluid flow, the research field can be categorized as continuous-flow and digital MMF. In continuous-flow MMF, fluids are supplied or manipulated in a continuous manner, where the fluids exist in a single phase as in the case of MHD

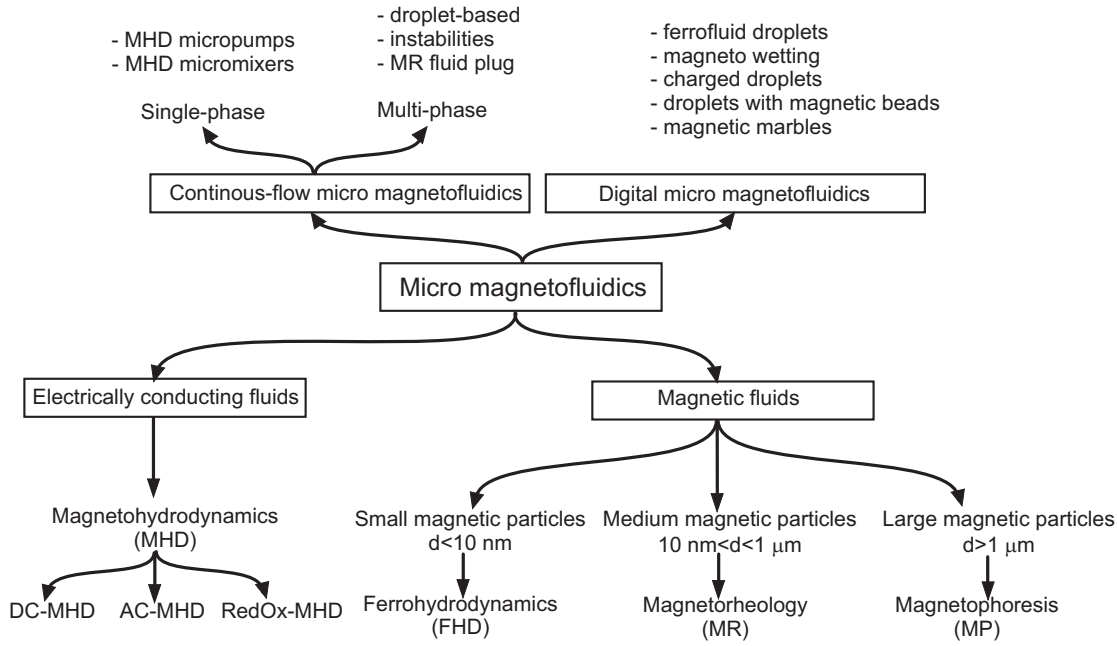


Fig. 2 Micro magnetofluidics, its subfields and representative applications. The line widths correspond to the number of references reviewed in this paper.

pumps and MHD mixers or in multiple phases such as emulsion. In digital MMF, fluids are manipulated as individual droplets or marbles, which are droplets with a protective coating of hydrophobic particles. Magnetic particles inside a droplet allow its control and manipulation using a magnetic field.

Following, fundamentals of magnetic forces in microscale, dimensionless numbers and their scaling laws are first discussed. Important phenomena are subsequently discussed according to the type of the fluid.

2 Fundamentals of micro magnetofluidics

2.1 Magnetic properties, field and forces

Magnetic force in microscale is generally well understood. All existing theories and models assume the magnetic material or the fluid as a bulk continuum and the force caused by a magnetic field gradient as a body force. A magnetic field is induced by free electric current \mathbf{J}_f and bound electric current \mathbf{J}_b . The set of Maxwell equations describing the magnetic field is:

$$\nabla \times \mathbf{H} = \mathbf{J}_f \quad (1)$$

$$\nabla \times \mathbf{M} = \mathbf{J}_b \quad (2)$$

$$\nabla \times \mathbf{B} = \mu_0(\mathbf{J}_f + \mathbf{J}_b) = \mu_0 \mathbf{J} \quad (3)$$

$$\nabla \cdot \mathbf{B} = 0 \quad (4)$$

where \mathbf{B} , \mathbf{H} , \mathbf{M} and $\mu_0 = 4\pi \times 10^{-7}$ are the flux density in Tesla (T), magnetic field strength in A/m, the local

magnetization in A/m and the permeability of vacuum in N/A^2 . The relationship between the flux density, the field strength and the local magnetization results from (1–3):

$$\mathbf{B} = \mu_0(\mathbf{H} + \mathbf{M}) = \mu_0(1 + \chi)\mathbf{H} \quad (5)$$

where χ is the susceptibility of the material. Materials with negative susceptibility ($\chi < 0$) are called *diamagnetic*. *Paramagnetic* materials have a positive susceptibility ($\chi > 0$). *Ferromagnetic* materials such as iron, cobalt, nickel and their compound with rare earth elements have large positive susceptibility ($\chi \gg 0$). In small ferromagnetic nanoparticles, magnetization can randomly flip direction under the influence of temperature. In the absence of an external magnetic field, their average magnetization is zero, this state is called *superparamagnetic*. In the presence of an external magnetic field, the nanoparticles are magnetized and becomes ferromagnetic. Balancing the magnetic energy and the thermal energy, a critical diameter for a ferromagnetic particle to be super paramagnetic can be estimated. Table 1 lists the critical diameters of ferromagnetic particles, below which the material is superparamagnetic as well as the critical **Curie** temperature, beyond which the material loses its net magnetization.

A magnetic field in a liquid medium can induce the following magnetic forces: magnetohydrodynamic force, magnetic gradient force, magnetization gradient force and magnetic interfacial force. While the first three forces are body forces, the last one is seen as an effec-

Table 1 Critical diameters of ferromagnetic particles

Material	Diameter (nm)	Curie temperature (°C)
Co	70	1130
Fe	14	770
Ni	55	358
Fe ₃ O ₄	128	585

tive surface force and can take advantage of the scaling law in microscale.

The Lorentz equation describes the force acting on a charged species with charge q moving with a velocity \mathbf{v} in an electric field \mathbf{E} and a magnetic field \mathbf{B} :

$$\mathbf{f}_{\text{Lorentz}} = q(\mathbf{E} + \mathbf{v} \times \mathbf{B}) \quad (6)$$

In the absence of an electric field, the sum of $q\mathbf{v}$ over a unit volume represents the current flux \mathbf{J} and the magnetic body force acting on the unit volume is:

$$\mathbf{f}_{\mathbf{B}} = \mathbf{J} \times \mathbf{B} \quad (7)$$

In the absence of both electric field and electric current, the force density acting on a magnetic fluid is calculated based on the magnetic energy density $e_m = -\mathbf{M} \cdot \mathbf{B}$. The magnetic force can then be derived as:

$$\begin{aligned} \mathbf{f} &= -\nabla e_m = -\nabla(\mathbf{M} \cdot \mathbf{B}) \\ &= (\mathbf{M} \cdot \nabla)\mathbf{B} + (\mathbf{B} \cdot \nabla)\mathbf{M} + \\ &\quad \mathbf{M} \times \nabla \times \mathbf{B} + \mathbf{B} \times \nabla \times \mathbf{M} \end{aligned} \quad (8)$$

Since no electric current exists, the Ampere law of (1,2,3) leads to $\nabla \times \mathbf{B} = 0$ and $\nabla \times \mathbf{M} = 0$, and the magnetic force density acting on a magnetic fluid is:

$$\mathbf{f} = (\mathbf{M} \cdot \nabla)\mathbf{B} + (\mathbf{B} \cdot \nabla)\mathbf{M} \quad (9)$$

In a nonuniform magnetic field, the force acting on a homogenous magnetic fluid is called the Kelvin body force[88]:

$$\mathbf{f}_{\nabla\mathbf{B}} = (\mathbf{M} \cdot \nabla)\mathbf{B} \quad (10)$$

In an inhomogeneous magnetic fluid with a gradient $\nabla\mathbf{M}$ a uniform magnetic field \mathbf{B} , the force acting on the magnetic fluid is:

$$\mathbf{f}_{\nabla\mathbf{M}} = (\mathbf{B} \cdot \nabla)\mathbf{M} \quad (11)$$

The gradient of magnetic moment is caused by a gradient of magnetic susceptibility, or concentration gradient of magnetic nanoparticles as well as paramagnetic ions.

In a two-phase system, the mismatch in magnetization \mathbf{M}_1 and \mathbf{M}_2 between the two fluids 1 and 2 leads to the Kelvin body force which can be expressed as the gradient of surface stress (the Maxwell stress tensor) and has the form[24]:

$$\begin{aligned} \mathbf{F}_s &= V\mathbf{f}_s \\ &= V[(\mathbf{M}_1 - \mathbf{M}_2) \cdot \nabla]\mathbf{B} \\ &= [(\mathbf{m}_1 - \mathbf{m}_2) \cdot \nabla]\mathbf{B} \end{aligned} \quad (12)$$

where \mathbf{m}_1 and \mathbf{m}_2 are the magnetic moments of fluid 1 enclosed in the volume V and the corresponding displaced fluid 2.

2.2 Dimensionless numbers and scaling laws

In traditional MHD, the interaction between the magnetic field and the flow field of a fluid with an electrical conductivity σ_{el} and permittivity μ is described by the magnetic Reynolds number [17]:

$$\text{Re}_m = \frac{\text{Advection of magnetic field}}{\text{Diffusion of magnetic field}} = \frac{ul}{\lambda} \quad (13)$$

where $\lambda = 1/(\mu\sigma_{\text{el}})$ is the diffusivity of the magnetic field, u is the velocity of the fluid and l is the characteristic length scale. In a system with a large magnetic Reynolds number, the field line is bent toward the flow direction. In micro magnetofluidics, a typical length scale of $l = 100 \mu\text{m}$, velocity of $u = 100 \mu\text{m/s}$ and magnetic field diffusivity of $\lambda = 1 \text{ m}^2/\text{s}$, the typical magnetic Reynolds number is $\mathcal{O}(\text{Re}_m) = 10^{-8}$. For comparison, the magnetic Reynolds number of a sun spot, of the earth core flow are $\mathcal{O}(\text{Re}_m) = 10^8$ and $\mathcal{O}(\text{Re}_m) = 10^2$, respectively. Typical magnetic Reynolds number of macroscale lab experiments and industrial metallurgy ranges from 10^{-3} to 10^{-1} . The low magnetic Reynolds number in microscale indicates that the flow of an electrically conducting fluid will not significantly alter the magnetic field. Compared to other microfluidic phenomena with the same flow condition and dimension, the diffusivity of magnetic field $\mathcal{O}(\lambda) = 1 \text{ m}^2/\text{s}$ is several orders of magnitude higher than the kinematic viscosity (momentum diffusivity) $\mathcal{O}(\nu) = 10^{-6} \text{ m}^2/\text{s}$ and diffusion coefficient (species diffusivity) $\mathcal{O}(D) = 10^{-9} \text{ m}^2/\text{s}$. In contrast to momentum and specie diffusion, diffusive transport of a magnetic field dominates over convection in microscale.

Another dimensionless number used in traditional MHD is the Hartmann number [17]:

$$\text{Ha} = \frac{\text{Lorentz force}}{\text{Friction force}} = Bl\sqrt{\frac{\sigma_{\text{el}}}{\eta}} \quad (14)$$

where η is the dynamic viscosity of the fluid. Since $\text{Ha} \propto l$, Hartman number decreases with miniaturization, indicating that Lorentz force does not scale favorably in microscale. The ratio between Lorentz force and inertial force is called the interaction parameter [17]:

$$\text{N} = \frac{\text{Lorentz force}}{\text{Inertial force}} = \frac{\sigma_{\text{el}}B^2l}{\rho u} \quad (15)$$

where ρ is the density of the fluid. The interaction parameter does not depend on the length scale. However, this number is proportional to the square of magnetic flux indicating the fast response of MHD flow when a strong magnetic field is applied.

Magnetic Bond number represents the ratio between magnetic force and surface tension force[25]:

$$\text{Bo}_m = \frac{\text{magnetic force}}{\text{surface tension force}} = \begin{cases} \frac{\mu_0 \chi_m l H^2}{\sigma} & (\text{below saturation}) \\ \frac{\mu_0 \phi \bar{M}_{\text{sat}} l H}{\sigma} & (\text{above saturation}) \end{cases} \quad (16)$$

where σ is the surface or interfacial tension, ϕ is the volume fraction of the magnetic particles in the fluid and \bar{M}_{sat} is the bulk saturation magnetization of the magnetic material. Magnetic Bond number represents the magnetic body force and scales unfavorably in microscale as in the case of Hartman number. The magnetic Laplace number represents the ratio between magnetic force and friction force:

$$\text{La}_m = \frac{\text{magnetic force}}{\text{friction force}} = \frac{\mu_0 H^2 \rho l^2}{\eta^2} \quad (17)$$

To apply the scaling law to magnetic particles suspended in a fluid, the diameter d of the magnetic particle is taken as the characteristic length. The ratio between the magnetic energy $E_m = mB = \frac{\pi}{6} d^3 MB$ with M the magnetization of the particle and other types of energy such as:

- thermal energy $E_{\text{th}} = k_B T$ with k_B the Boltzmann constant and T the temperature,
- gravitational potential energy $E_g = \Delta \rho g h \pi d^3 / 6$ with g the gravitational acceleration and h the relative height to a surface,
- magnetic dipole potential energy $E_d = \frac{\mu_0 \pi M^2 d^3}{72(\delta/d + 1)^3}$ with δ the distance between two neighboring particles and
- frictional energy $E_f = 3\pi \eta d^2 u$

lead to a number of magnetofluidic dimensionless numbers, which are called here stability numbers S to estimate the relative stability of the magnetic particles.

The thermal stability number also called the Langevin parameter:

$$S_{\text{th}} = \frac{E_m}{E_{\text{th}}} = \frac{\pi}{6} \frac{MBd^3}{k_B T} \quad (18)$$

is proportional to d^3 . That means miniaturization leads to diminishing influence of magnetic energy. If the particles are small enough, thermal energy dominates leading to the superparamagnetic property mentioned above.

The sedimentation stability number:

$$S_s = \frac{E_m}{E_g} = \frac{MB}{\Delta \rho g h} \quad (19)$$

does not scale with miniaturization because both gravitational and magnetic forces are body forces. Since the

two forces are comparable, magnetic force can replace buoyancy force in micro gravity condition. This feature has been used for free convective cooling in space flight.

The dipole stability number:

$$S_d = \frac{E_m}{E_d} = 12 \frac{B}{\mu_0 M} \left(\frac{\delta}{d} + 1 \right)^3 \quad (20)$$

has two length parameters, the particle diameter d and the distance between the particles δ . The dipole stability number is large if the diameter of the particle is small. A large particle reduces S_d leading to the dominance of dipole interaction. The magnetic particles are then able to self-assemble forming supraparticle structure (SPS) and leading to magnetorheological behavior.

The magnetophoretic stability number:

$$S_{\text{mp}} = \frac{E_m}{E_f} = \frac{1}{18} \frac{MBd}{\eta u} \quad (21)$$

decreases with decreasing particle diameter. That means, small magnetic particles cannot be separated by magnetic force due to the dominant friction force.

3 Electrically conducting fluids

MHD for pumping and mixing of electrically conducting fluids in microfluidics was investigated and implemented early. Qian and Bau gave a comprehensive review on MHD-based microfluidics [68]. In addition to Maxwell's equation and continuity equation, the flow of a conducting fluid in a magnetic field is governed by Navier-Stokes equation with the additional term of Lorentz force:

$$\rho \frac{D\mathbf{u}}{Dt} = -\nabla p + \eta \nabla^2 \mathbf{u} + \mathbf{J} \times \mathbf{B} \quad (22)$$

Solving the above equation for a two-dimensional parallel plate model leads to the velocity distribution of the MHD flow [17]:

$$u = u_0 \left[1 - \frac{\cosh(\text{Ha}y/h)}{\cosh(\text{Ha})} \right] \quad (23)$$

For a small Hartman number, the velocity distribution approaches that of pressure driven flow $u = u_0 [1 - (y/h)^2]$. For a large Hartmann number, the velocity distribution flattens with a boundary layer called Hartman layer $\delta = \sqrt{\rho \nu / \sigma B^2}$. In most microfluidic applications, the conducting fluids are electrolyte solutions with low conductivity corresponding to a low Hartman number. Therefore, a velocity profile similar to that of pressure driven flow can be expected for MHD flow in microchannels. Liquid metals and plasma are not relevant for microfluidics. The two main challenges posed by electrolyte solutions are the low conductivity and the electrochemistry associated with the use of electrodes

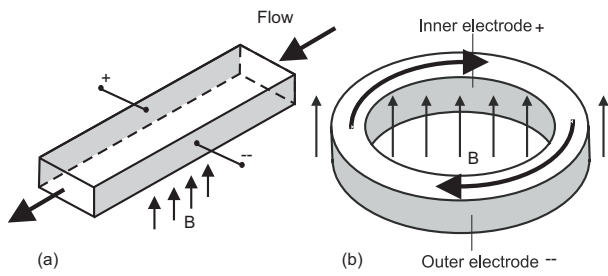


Fig. 3 Basic configurations of MHD micropumps: (a) straight channel; (b) annular channel.

in direct contact with the solution. However, the ions generated by reduction/oxidation reactions at the electrode could lead to interesting flow phenomena that can be utilized for mixing and pumping.

Jiang and Lee [34] reported a MHD micropump made in a straight silicon microchannel, Fig. 3(a). The pump worked with a maximum flux density of 0.44 T generated by a permanent magnet and a voltage from 10 to 60 V. Zhong et al. [96] implemented the MHD concept in an annular microchannel (Fig. 3(b)) for pumping mercury, saline solution and deionized water. Due to the high conductivity of mercury, operation at relatively high Hartmann number and high magnetic Reynolds number is possible even in the microscale. A serious problem of the above DC-MHD micropump is the generation of hydrolysis bubbles at the electrodes. To avoid the problem of bubbles trapped in the flow channel, Homsey proposed a design with electrodes placing outside the flow channel. The electric field is applied through a small gap connecting the reservoirs with electrodes and the flow channel. To increase the flow rate, Homsey et al. [33] used a strong magnet of 7 Tesla. A linear relationship between the flow rate and the applied voltage was found. Nguyen and Kassegne [56] reported a similar bubble trapping design allowing operation with relatively high voltage and flow rate. Recently, Kang et al. [37] proposed a DC-MHD with planar electrodes. However, the pumping effect was not as strong as that with conventional electrodes on the side wall.

Bubble generation can be avoided if both AC magnetic field and AC electric field are used. The AC signals are synchronized so that the flow direction remains unchanged [44]. Since the field strength of an electromagnet is much lower than a permanent magnet of the same size, only a relatively small flow rate can be achieved with an AC-MHD micropump. The same concept of AC-MHD was implemented in a microfluidic network, where each branch is driven by a MHD pump [45]. Bubbles can also be avoided by keeping the voltage below the standard potential of water electrolysis of 1.23 V. Leventis and Gao [46] utilized reduction/oxidation (RedOx) reaction at the electrodes to supply the ions. High

ion flux generated by Faradaic charging can be achieved at low voltage without damaging the electrodes. The Faradaic charging process occurs at the interface between the electrode and the solution. A chemical species gains or loses electrons leading to a flux ions to maintain the neutral charge condition. An annular design based on the AC-MHD concept was reported by West et al. [87]. The closed loop design and Taylor dispersion promote fast mixing in this AC-MHD pump. Eijkel et al. [22] reported another AC-MHD pump with annular design. The pump and electrode are formed by a 30- μm thick gold layer deposited on glass.

Figure 4 shows the typical Hartman numbers of the above MHD pumps versus the magnetic Reynolds numbers as well as the Reynolds numbers $Re = \rho ul/\eta$. The solid lines are the power fitting functions. The parameters for calculating the Hartman number and magnetic number are taken from the respective papers. If the information is not available, data of 1M NaCl solution is assumed. Since the Lorentz force is the driving force, the Hartman number correlates with the Reynolds number. Large Hartman number and corresponding high Reynolds number can be achieved with highly conducting fluid such as mercury or abundant supply of ions as in the case of RedOx-MHD pump. The high Reynolds numbers in these cases are consistent with the unstable and turbulent flows observed in the experiments. Effective MHD pumping schemes are located at the lower right corner of Ha-Re parameter space. The data in Figure 4(a) show that the circular loop is a good design because the the entire closed-loop microchannel works as a pump against a zero back pressure. Furthermore, gas bubbles will absorb all the energy induced by the Lorentz force. Thus, micropumps with AC-MHD and designs that can avoid bubble formation also belong to those of better performance. The higher flow with high Hartman number agrees with the correlation shown in Fig. 4(b). The small magnetic Reynolds numbers of the reported work confirm the conclusion from scaling law that the flowing conducting liquid in micro magnetofluidics will not have any effect on the magnetic field. For modeling purposes, it is safe to assume that the magnetic field is not affected by the flow of the conducting fluid. The magnetic field and the flow field can be decoupled and solved separately.

4 Magnetic fluids

Magnetic fluids are referred here to liquids with suspended magnetic particles. The particles can be as small as free ions of a paramagnetic aqueous solution. Dissolved paramagnetic ions such as Mn^{2+} , Cu^{2+} and rare

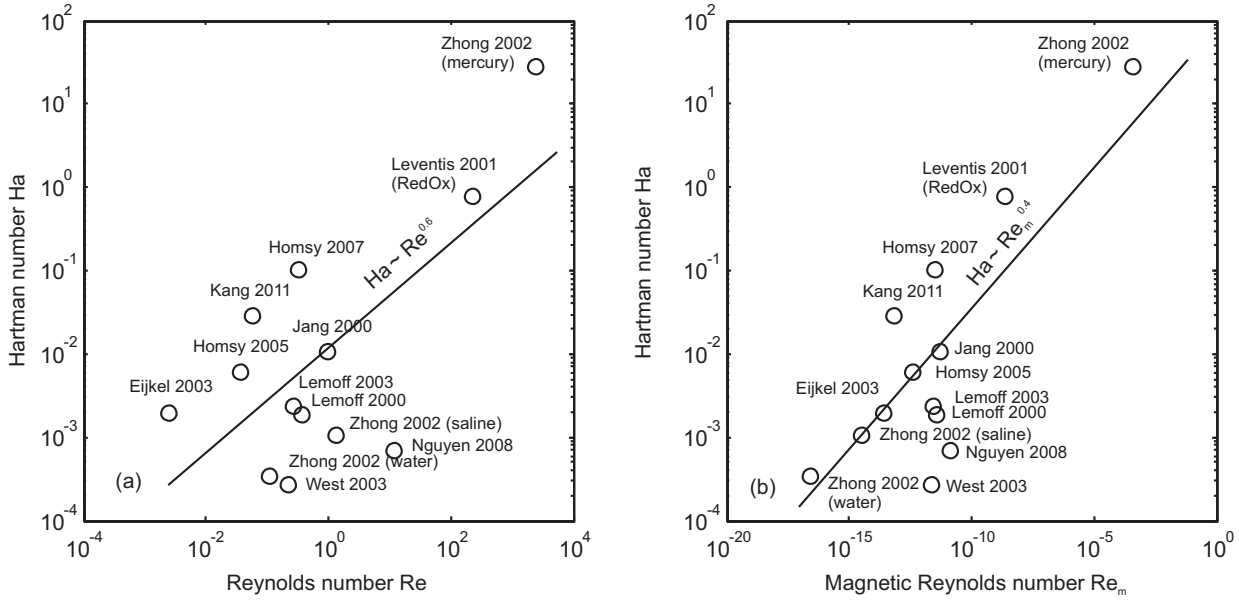


Fig. 4 Hartman numbers of reviewed MHD micropumps versus Reynolds number (a) and magnetic Reynolds number (b).

earth ions can significantly change the magnetic susceptibility of an aqueous solution. Larger magnetic nanoparticles can be stabilized in a solution with the help of a surfactant and the dominant thermal energy. Since the magnetic particles are well suspended in the carrier fluid, the entire magnetic fluid is treated as a continuum and are discussed under the section on ferrohydrodynamics (FHD). For larger particles, dipole interaction is important leading to magnetoviscous phenomena. In this case, the magnetic fluid can still be treated as a continuum and will be discussed under the section on magnetorheology (MR). For very large magnetic particles, the particles should be treated as discrete entities in a carrier fluid. The manipulation of magnetic particles in diamagnetic carrier fluid and diamagnetic particles in magnetic carrier fluid are discussed under the section on magnetophoresis (MP).

4.1 Ferrohydrodynamics

The Navier-Stokes equation formulated with an additional term of magnetic gradient force reads [71]

$$\rho \frac{D\mathbf{u}}{Dt} = -\nabla p + \eta \nabla^2 \mathbf{u} + (\mathbf{M} \cdot \nabla) \mathbf{B} \quad (24)$$

The above equation reveals that either a gradient of the magnetic field or of the magnetization field of the ferrofluid is needed to move the fluid against a pressure gradient. Mao and Koser [54] reported numerical and experimental results of single-phase ferrofluid using a traveling magnetic field. **The pumping frequency is on the order of 1 kHz. Since both Brownian and Neel**

relaxation times [71] of the magnetic nanoparticles correspond to a much higher frequency, this relatively low frequency may probably be caused by the formation of larger particle chains [53]. The pump can only achieve a pressure head of few Pascals at an extremely high driving current of 10 A. Furthermore, the high current induces heating, which in turn affect the susceptibility and the magnetization of the ferrofluid. The magnetization degrades with increasing temperature. Beyond the critical Currie temperature (Table 1), the particles lose their net magnetization. A temperature gradient leads to a gradient of magnetization and a gradient of magnetic body force that can drive the ferrofluid in a microchannel. This phenomena was called by Love et al. the *magnetocaloric* effect [52]. The additional body force experienced by the fluid from (11) has the magnetocaloric form [52]:

$$\mathbf{f}_{mc} = \frac{1}{2} \left(\mathbf{B} \cdot \frac{\partial \mathbf{M}}{\partial T} \right) \nabla T \quad (25)$$

Love et al. used ferrofluid based on $\text{Mn}_{0.5}\text{Zn}_{0.5}\text{Fe}_2\text{O}_4$ that has a low Currie temperature of 150°C . Li et al. [47] and Lian et al. [48] used a similar Mn-Zn ferrite based fluid to realize a cooling loop using magnetocaloric pumping. The magnetic field was provided by a NdFeB permanent magnet. This pumping concept was implemented in a heat exchanger for cooling applications [90]. Pal et al. used an electromagnet to provide a homogeneous magnetic field in the flow channel [62], Fig. 5(a).

In a two-phase system, ferrofluid forms a droplet or a plug which works as a piston to drive the other immiscible phase. Hatch et al. [32] used ferrofluid plugs as

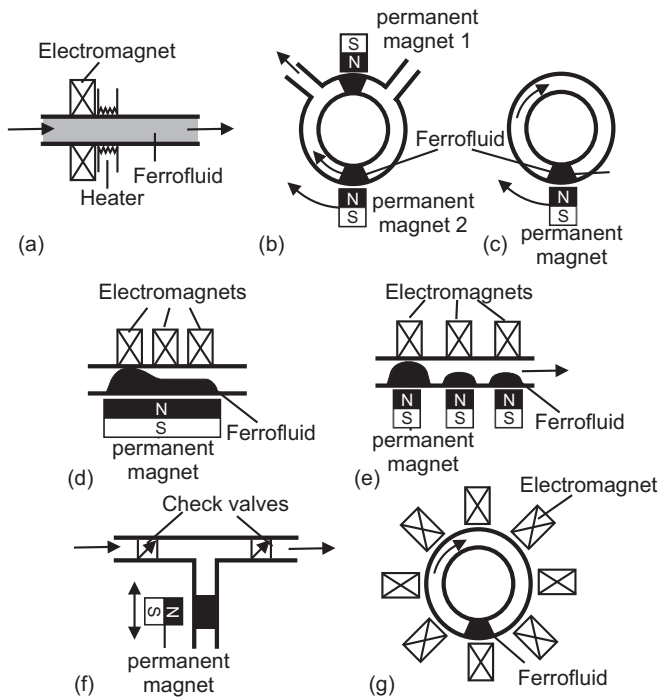


Fig. 5 Concepts of ferrohydrodynamic micropumps: (a) magnetocaloric pump [62]; (b) annular pump with two ferrofluid plugs [32]; (c) annular pump with one ferrofluid plug [77]; (d) peristaltic pump [4]; (e) pump with three ferrofluid valves [5]; (f) pump with check valves and ferrofluid piston [92]; (g) stepper ferrohydrodynamic pump [58].

both valve and piston to realize a micropump, Fig. 5(b). Two external permanent magnets were used. A stationary magnet to hold a ferrofluid plug in place working as a valve. A second magnet moves in a loop working as a piston to pump another immiscible phase such as water in the microchannel. Ahn et al. [3] used a rotating external magnet to drive the ferrofluid plug. Sun et al. [77, 78, 76] used the same concept to drive liquid in a closed circular microchannel loop, Fig. 5(c). A single permanent magnet can be used for pumping sample liquid in multiple concentric microchannel loops. Hartshorne et al. [31] reported a design with three ferrofluid plugs, two working as valves and one as the piston. Synchronizing the motions of the pistons and the two valves allow pumping of both air and water. The pump cycle of 30 minutes makes the pump not practical for most applications. Ando et al. [4] used a permanent magnet to keep a ferrofluid plug in a glass capillary at a fixed location, Fig. 5(d). Actuating coils around the capillary causes a peristaltic motion of the plug driving the immiscible phase. The team used the same concept to control three separate ferrofluid plugs in a glass capillary. Synchronizing the actuation of the three plugs leads to pumping of the nonmagnetic immiscible fluid [5], Fig. 5(e). Yamahata et al. [92] used a ferrofluid as

the piston to drive a check valve micro pump, Fig. 5(f). The reciprocating motion of the ferrofluid plug is induced by an external permanent magnet. Nguyen et al. used multiple solenoid magnets around a loop and a ferrofluid plug to realize a stepper ferrohydrodynamic micropump [58], Fig. 5(g).

Figure 6(a) depicts the magnetic Bond number of the above ferrohydrodynamic pumps versus the corresponding Reynolds number. The filled circles represent the single-phase magnetocaloric pumps, where the ferrofluid itself is pumped. The white circles represent multi-phase pumps where the ferrofluid plug works as an actuator for a conventional mechanical pump. We can clearly observe the difference in behavior of these two pump types in the B_{om} - Re space. Since the magnetocaloric concept relies on the temperature dependence of the ferrofluid, the limited range of driving temperature gradient leads to a narrow range of the Reynolds number, which represents the maximum flow rate the pump can achieve. The strength of the magnetic field represented by the magnetic Bond number does not affect the Reynolds number. In contrast, the mechanical pumps using a ferrofluid plug as an actuator have a wide range of Reynolds number indicating that the pump performance depends on other parameters such as pumping frequency and the viscosity of pumped liquid. The stroke volume of these pumps does not depend on the magnetic field strength because the ferrofluid is already working in a saturated state. Another observation from Fig. 6(b) is that the magnetic Bond number are relatively high. That means magnetic body force dominates over interfacial tension. Using a ferrofluid plug as an actuator requires this condition because magnetic force should overcome both surface tension and friction to move the plug. In the case of the pump reported by Ando et al. [4, 5] the magnetic force should be large enough to deform the liquid interface, thus a large magnetic Bond number is needed.

A micropump with an actuating ferrofluid plug is considered as a multiphase system. Recently, the formation, manipulation and application of ferrofluid droplets in an immiscible fluid have attracted great interests from both microfluidics and magnetic fluid communities. In the macroscale, the magnetic Bond number is large due to the dominant magnetic force. For instance, a normal magnetic field applied to the free surface of a ferrofluid leads to the formation of free-standing spikes called Rosensweig instability [16]. Research on multiphase systems involving ferrofluid was mainly focused on the instability pattern of a ferrofluid droplet under different conditions of magnetic field [69], [14].

In microscale, the smaller magnetic Bond number makes droplets more stable against the magnetic force.

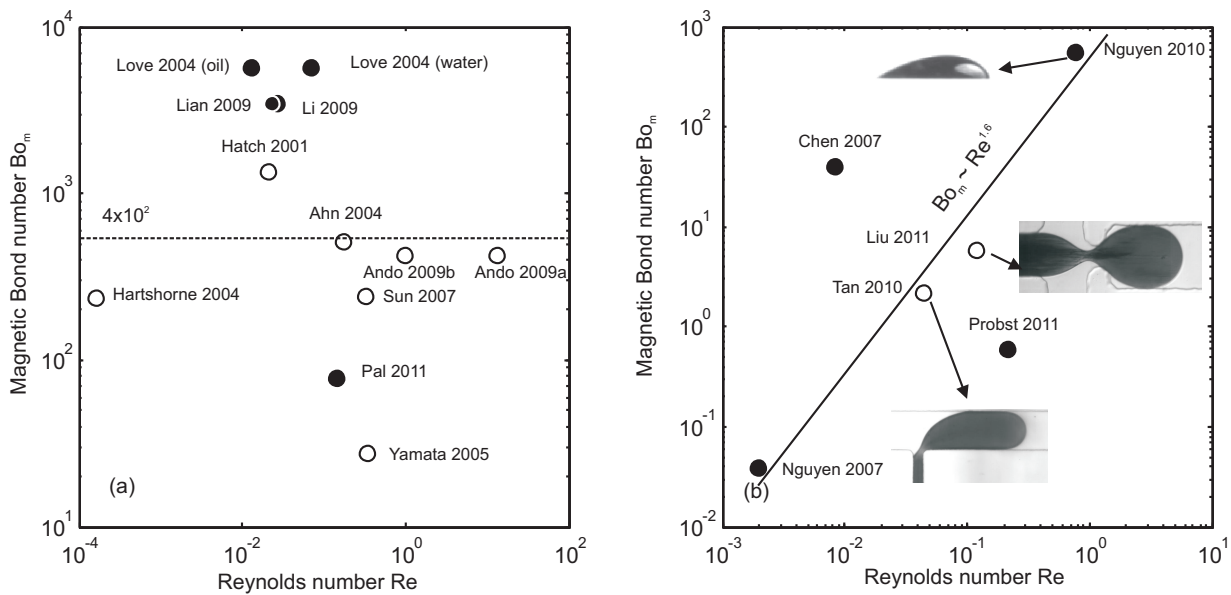


Fig. 6 Bond numbers versus Reynolds number of (a) reviewed FHD micropumps (the filled circles \bullet and the circle \circ represent the single-phase and multi-phase FHD micropumps, respectively); (b) reviewed droplet-based systems (For a sessile droplet, the diameter and properties of the ferrofluid is taken for calculating the Reynolds number. For the droplet formation process, the Reynolds number is calculated based on the properties of carrier fluid and the hydraulic diameter of the microchannel).

The formation of ferrofluid droplets can be realized with common methods of droplet-based microfluidics such as shear and pressure driven formation at a T-junction or a flow-focusing junction. Since ferrofluid is a special class of nanofluid, even without an applied magnetic field, the droplet formation of ferrofluid is affected by the nanoparticles and their surfactant. Nanoparticles at the fluid interface reduce the interfacial tension leading to the formation of smaller droplets as compared to those of the pure carrier fluid under the same condition [55]. Chen et al. only used the magnetic body force to form ferrofluid droplets through an orifice [13]. Tan et al. combined pressure-driven flow with the magnetic force to control the droplet formation process at a microfluidic T-junction [81]. The magnetic field gradient was generated by an external permanent magnet. The direction of the induced magnetic force is controlled by the relative position between the the T-junction and the magnet. Both direction and magnitude of the magnetic force can be used to tune the size of the formed ferrofluid droplets. In a uniform magnetic field, the magnetic body force disappears due to the missing field gradient. However, the mismatched magnetic susceptibilities of the ferrofluid and the immiscible phases lead to a surface force (12) that can be used for controlling the formation process of ferrofluid droplets [51]. Under a uniform magnetic field in flow direction, the stretching of the fluid interface at the flow-focusing junction leads to the formation of larger ferrofluid droplets [50]. In a T-junction, the uniform magnetic field has the op-

posite effect, the formed droplet becomes smaller [80]. The size of the droplet in a ferrofluid emulsion can be adjusted by flow rates, flow rates ratio, pressures and temperature [57]. A ferrofluid emulsion system can have interesting behavior similar to a magnetorheological fluid when exposed to a magnetic field [49]. Figure 6(b) shows the characteristic magnetic Bond number and Reynolds number of the above examples on formation of ferrofluid droplets. While a large magnetic Bond number is needed for forming droplets with magnetic force only, the magnetic Bond number increases with increasing Reynolds number for the combination of hydrodynamic and magnetic forces.

A stand-alone magnetic droplet can be manipulated with an external magnetic field. Nguyen et al. use planar microcoils to control the one-dimensional movement of a ferrofluid droplet suspended in silicone oil [59]. The magnetic force is large enough to overcome the friction force and the deformation of the droplet [59, 8]. The concept was later extended to two-dimensional manipulation using four planar microcoils [9]. The microcoils can only produce a magnetic field on the order of 1 mT. Thus an external permanent magnet was needed to magnetize the nanoparticles in the ferrofluid droplet. Probst at al. used four stronger external solenoid electromagnets with a maximum field of 200 mT for controlling the movement of the ferrofluid droplet [67]. Due to the strong decay and the larger distance between the magnet and the droplet, the actual magnitude of the actuating magnetic field is only few mT. With digital

image acquisition and processing, a closed-loop control of the droplet path can be achieved with an average error of about 1/3 of the droplet diameter.

A sessile magnetic droplet on a planar surface represents a convenient platform for digital microfluidics. Chen et al. [12] investigated Rosensweig instability of a sessile ferrofluid droplet in a uniform field and a large magnetic Bond number. Nguyen et al. [60] utilized a smaller nonuniform magnetic field to deform the sessile ferrofluid droplet and observed an decreasing apparent contact angle with increasing magnetic field. This phenomenon was termed as *magnetowetting*, which later was confirmed by Berim and Ruckenstein using density functional theory of simple fluids [7]. Based on this model, the contact angle increases with increasing uniform magnetic field approaching an asymptotic value, Fig. 7(a). In a nonuniform field, the contact angle first increases with increasing magnetic field and then decreases almost linearly with the increasing field strength, Fig. 7(b). A sessile droplet can be manipulated by moving the external magnet. Since the magnetic force needs to overcome the capillary force and friction force, the motion of the droplet depends on its size, the field strength and the motion speed. An operation space for a moving sessile droplet was derived with these three parameters [60]. Magnetic beads with size ranging from one to tens of micrometers are not homogeneously distributed in the droplet, and can be easily clustered or extracted from the liquid under a strong magnetic field.

The different behaviors of contact angles in a uniform and non uniform field may potentially lead to a new manipulation concept based on magnetowetting. The nonuniform magnetic field can be generated with an array of microcoil. Together with an overlapping uniform field, switching the coils and the local nonuniform field could move a sessile ferrofluid droplet around. Another approach for magnetowetting is using magnetically controllable surface. Zhou et al. [97] created a nano structured surface made of tiny polymeric tubes with embedded superparamagnetic Fe_3O_4 nanoparticles. The tubes respond to an external magnetic field leading to the change of the contact angle of the droplet, Fig. 7(c).

Liquid marbles are formed by self-assembly of hydrophobic particles at the liquid/air interface of a liquid droplet[6]. Since the hydrophobic particles prevent the direct contact between the liquid and a surface, a liquid marble represents a perfect non wetting system with a contact angle close to 180° . Ferrofluid can be used to form a magnetic marble [10]. While a sessile ferrofluid droplet dragged by a moving permanent magnet slides on a smooth surface (Fig. 7(d)), a ferrofluid

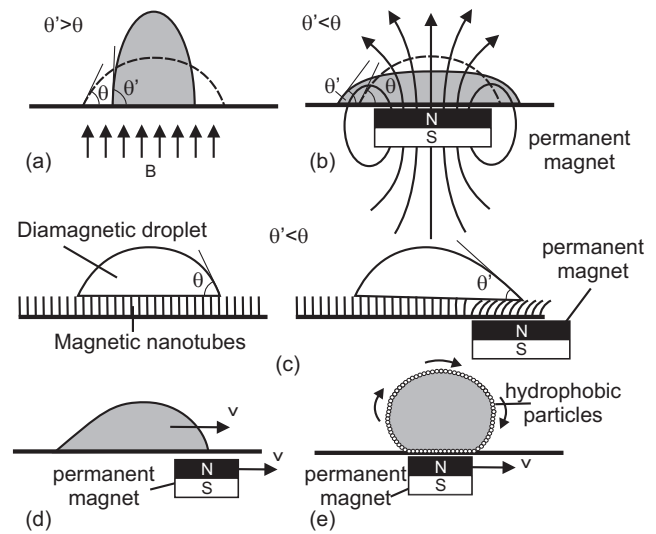


Fig. 7 Magnetowetting phenomena: (a) in a uniform magnetic field; (b) in a nonuniform magnetic field; (c) with magnetically controllable surface; (d) sliding motion of a sessile ferrofluid droplet; (e) rolling motion of a ferrofluid marble.

marble rolls under the same condition (Fig. 7(e)). A magnetic marble can also be formed with a diamagnetic fluid and hydrophobic magnetic particles. Zhao et al. [95] synthesized highly hydrophobic Fe_3O_4 nanoparticles for making magnetic water marbles. The marble can be manipulated with an external permanent magnet. Since the coating particles can be manipulated, this type of marble allows the hydrophobic coating to open and to close reversibly leading to controllable merging of two marbles. Marble with magnetic coating also rolls after a moving permanent magnet [91].

4.2 Magnetorheology

A magnetorheological fluid (MR fluid) consists of larger magnetic particles on the order of 100 nm to $10\ \mu\text{m}$. The particles are too large to keep them suspended by Brownian motion. Under a magnetic field, magnetic particles align under dipole interaction and form chains and structures called supraparticle structures (SPS). These chains restrict the fluid flow perpendicular to the magnetic field, increasing the apparent viscosity of the fluid. If the field is strong enough, the MR fluid behaves as a viscoelastic solid. A ferrofluid emulsion system also shows a similar behavior, which can be explained theoretically [49].

Despite the interesting properties of magnetorheological fluids, not many applications were reported in the literature. The magnetically controllable viscosity of MR fluid can be used for separation of large molecules in microchannels. The change in viscosity helps to solve the problem of filling microchannels with highly viscous

gel matrix. The separation channel is first filled with the less viscous fluid in the absence of a magnetic field. Once the fluid is in place, the magnetic field is turned on and changes it into a solid separation matrix. Doyle et al. [20] utilized the SPS assembled in a microchannel as the separation matrix for deoxyribonucleic acid (DNA). Only a relatively small magnetic field of around 10 mT is required to turn the magnetic liquid into the matrix. The spacing of the matrix can be tuned with particle size and concentration.

MR has similar properties as electrorheological (ER) fluids whose viscosity is changed under an applied electric field [94]. Similar to MR fluids, dipole interactions allow the formation of particle columns and the increase of the viscosity. As reported by Niu et al. [61] for ER droplets, MR droplets can be formed and manipulated by a magnetic field. The manipulation of these "smart" droplets would allow the implementation of more complex microfluidic functions such as logic gates [84].

4.3 Magnetophoresis

In a magnetic field gradient, a magnetic bead driven by the gradient force moves along the gradient. The phenomenon is called magnetophoresis. Formulating equation (12) for a magnetic particle, the force acting on a particle in a carrier fluid with mismatching susceptibilities is [29]:

$$\mathbf{F}_m = \frac{V(\chi_p - \chi_f)}{\mu_0} (\mathbf{B} \cdot \nabla) \mathbf{B} \quad (26)$$

where V is the volume of the particle. Since the magnetic force is acting based on the mismatch of susceptibilities, both manipulating a magnetic particle in a diamagnetic fluid and a diamagnetic particle in a magnetic fluid are possible. The term $(\mathbf{B} \cdot \nabla) \mathbf{B}$ is called the magnetic force field. Magnetic field of microcoils are on the order of few mT, two orders of magnitude smaller than that of a permanent magnet. As results, magnetophoretic velocity induced by a coil is about four orders of magnitude smaller than that generated by a permanent magnet. Since both the magnetic field and the field gradient contribute to the strength of the magnetic force, overlapping an external uniform magnetic field with a local nonuniform magnetic field of a microcoil would result in a strong local magnetic force. Balancing the magnetic force and the friction force of a spherical particles $\mathbf{F}_f = 3\pi\eta d\mathbf{u}$, the magnetophoretic velocity can be estimated as [28]:

$$\mathbf{u} = \frac{d^2(\chi_p - \chi_f)(\mathbf{B} \cdot \nabla) \mathbf{B}}{18\mu_0\eta} = \frac{1}{\mu_0} \zeta (\mathbf{B} \cdot \nabla) \mathbf{B} \quad (27)$$

where $\zeta = d^2(\chi_p - \chi_f)/18\eta$ is called the magnetophoretic mobility. For the same magnetic force field, the magnetophoretic velocity scales with the square of the particle size. The smaller the particle, the slower is the velocity. Since the magnetophoretic velocity is also proportional to the magnetic gradient, the small size in microfluidics and the design of sharp magnetic poles [2] can help to increase magnetophoretic velocity.

The dependence of magnetophoretic velocity on the size and magnetic susceptibility allows the separation of diamagnetic and magnetic particles [65] as well as of magnetic particles with different sizes [64], Fig. 8(a). Han and Frazier [30] utilized a ferromagnetic wire made of electroplated NiFe alloy in a microchannel to generate a magnetic field gradient and consequently a magnetic force field, Fig. 8(b). The field was strong enough to separate paramagnetic red blood cells and diamagnetic white blood cells. With multiple stages, the sorting efficiency of this concept was improved significantly [36], Fig. 8(c). The difference in magnetophoretic velocities results in trajectories with different angles. Adams et al. utilized this phenomenon and the effect of magnetic force field around a ferromagnetic wire to separate cells tagged to magnetic beads with different susceptibilities and sizes [1], Fig. 8(d). Kang and Park [39] utilized the sharp poles of the saw-tooth ferromagnetic structure to generate the magnetic field gradient, Fig. 8(e). The corresponding magnetic force field was used to trap iron-contaminated carbon nanotubes. Smistrup et al. [74] used integrated permalloy structures on both sides of the flow channel to separate magnetic beads. Kang et al. [38] further improved the sensitivity of magnetophoretic separation by using a gradient of susceptibility generated by diffusive mixing of gadolinium paramagnetic diethylenetriamine-pentaacetic acid (Gd-DTPA). At a location along the concentration gradient, where the susceptibility of the particle matches with that of the solution, the magnetophoretic force is zero and the particle stays focused at this location. Since the concept is similar to isoelectrophoresis, this technique was called by Kang et al. isomagnetophoresis [38], Fig. 8(f). Krishnan et al. [42] combines magnetophoresis with dielectrophoresis to separate magnetic beads.

Besides ferromagnetic structures, current conducting electro magnet in form of microcoils [75] or micro stripes [41][19] (Fig. 8(g)) also have been used for magnetophoretic separation. The field strength and field gradient will be improved if the field lines of a microcoil are trapped by a ferromagnetic core. Choi et al. [15] reported the integration of an electromagnet based on a planar microcoil and a permalloy yoke. The same group reported the fabrication of a more complex integrated solenoid electromagnet with NiFe core [70].

Magnetophoretic effect also applies to diamagnetic particles in a paramagnetic solution. Watarai and Namba [85] observed magnetophoretic migration of polystyrene particles in manganese(II) chloride (MnCl_2) solution.

Magnetophoretic transport of particles is more challenging than magnetophoretic separation, because in the later case the particles are transported by the fluid flow. Without a flow, the magnetic force is the sole driving force for the magnetic beads. In general, the same concepts used for magnetic droplets can be used for magnetic particles. Magnetic particles are dragged by a moving external permanent magnet (Fig. 5(a)) or by an array of electromagnets [35], Fig. 5(g). Lee et al. [43] realized an electromagnetic trap by two pairs of stripes with opposing currents, Fig. 8(h). Wirix-Speetjens et al. [89] used saw-tooth current conductor to trap and transport particles, Fig. 8(j). Plouffe et al. [66] used a simple current conductor parallel to the flow channel to separate and trap magnetic particles. Deng et al. used micro stripes to locally trap the particles. Sequential activation of neighboring traps allows the transport of magnetic particles [18], Fig. 8(k).

More control over magnetophoresis can be achieved, if the particle is designed to have a more complex shape than the usual sphere. In this case, the particles can be considered as self-propelling devices or micro/nanobots. Kline et al. [40] fabricated a $1.5 \mu\text{m} \times 400 \text{ nm}$ nanorod by alternate electroplating of platinum, nickel and gold. While oxygen bubbles generated by catalytic reaction of H_2O_2 at the platinum end provide propulsion, the nickel stripes allows remote magnetic control. Burdick et al. [11] demonstrated that such as magnetically controllable nanobot can be attached to a cargo (polystyrene bead coated with iron oxide) and move in a microchannel network.

Tierno et al. [83][82] assembled two paramagnetic beads with different diameters of $2.8 \mu\text{m}$ and $1 \mu\text{m}$. The beads are linked by a 8-nm long cDNA strand and form a paramagnetic asymmetric doublet. A rotating AC magnetic field was generated by two external electromagnets. A third electromagnet generates a stationary magnetic field. The induced rotation of the doublet results in a translation on the surface of a glass plate. The direction of the motion can be controlled by the current direction in the electromagnets. Dreyfus et al. [21] used a similar technique to link up magnetic beads to a flexible chain. The external rotating magnet induces a beating motion mimicking flagella of spermatozoa. The speed and direction of the motion can be controlled by the external magnetic field. Another strategy to translate rotational motion into translational motion is using chiral structures such as helical and screw-shaped particles. Zhang et al. [93] fabricated a structure with

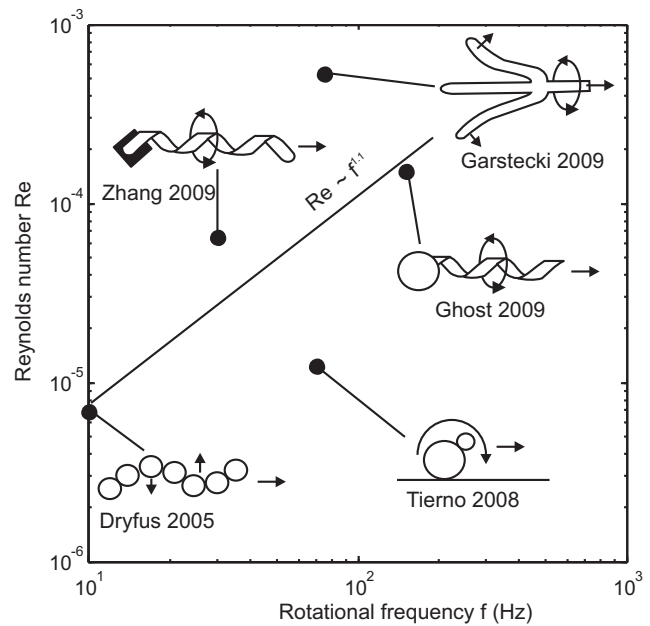


Fig. 9 Typical Reynolds number of magnetic micro swimmer versus corresponding rotational frequency of the driving magnetic field (The Reynolds number is calculated based on the length of the structure, its velocity and the properties of the surrounding fluid).

a softmagnetic head and a helical tail. The structure can swim with a speed proportional to the rotational frequency of the magnetic field. Ghost and Fisher [27] fabricated a screw-shaped structure with a spherical silica head and silicon oxide tail. Half of the structure is coated by a layer of cobalt which is subsequently magnetized. Garstecki et al. [26] fabricated magnetic micro swimmers in PDMS by mixing the prepolymers with magnetic particles and curing under a magnetic field. The resulting planar PDMS structures has therefore a permanent magnetic moment. An external uniform rotating magnetic field twisted the structure into helical symmetry and allowed it to propels in a translational manner. This concept mimics microorganisms that use rotational flagella and cilia to swim. Figure 9 summarizes the typical parameters of the above magnetic micro swimmers. If the magnetic torque is strong enough for the swimmer to follow the rotation of the magnetic field, the swimming velocity is almost proportional to the rotational frequency.

5 Conclusions and perspectives

The above review presents the state of the art of the field micro magnetofluidics. Three basic observations are made with the above reviewed works. First, micro magnetofluidics is not only about magnetic interactions of flow in microchannels, but also about behaviour and

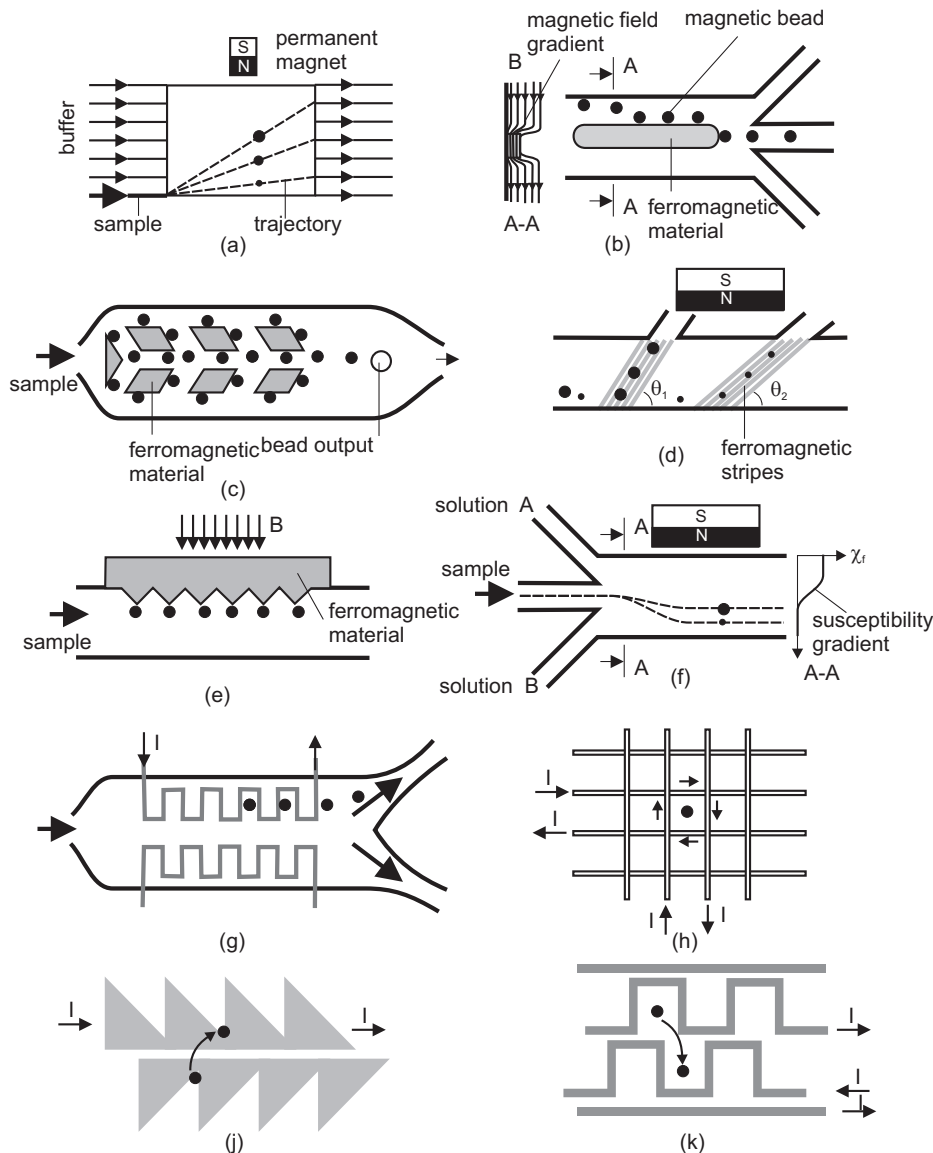


Fig. 8 Manipulation concepts based on magnetophoresis: (a) free-flow magnetophoresis [65]; (b) sorting with magnetic gradient induced by a ferromagnetic structure [30]; (c) multi-stage sorting with magnetic gradient induced by a ferromagnetic structure [36]; (d) sorting with ferromagnetic stripes [1]; (e) trapping with magnetic gradient induced by sharp poles [39]; (f) sorting with a gradient of susceptibility [38]; (g) sorting with electromagnetic stripes [35]; (h) trapping transport with wire loop created by addressable current conducting lines [43]; (i) trapping and transport with saw-tooth conducting wires [89]; (k) trapping and transport with meandering conducting wires [18].

flow around nano/microscopic objects. Second, most of the current works focus on the use of magnetism to manipulate fluid flow or movement of particles in a fluid. The other pathway of the interaction, using fluid flow to manipulate magnetic field, is generally neglected. Third, the general reception of magnetic force as body force prevents the further investigation and application of magnetowetting.

As mentioned above, the small Hartman number in most micro magnetofluidic applications does not allow a flowing conducting fluid to affect the magnetic field passing through it. However, the use of liquid met-

als with high conductivity would allow the increase of Hartman number. Although mercury has been used for MHD actuation, the availability of other liquid metals and metal alloys with low melting temperature would allow the use of liquid metals in microchannels [72]. A magnetic field can be generated with a liquid metal electromagnet [73]. Magnetic field can be manipulated with a multiphase system with mismatched magnetic susceptibility. There are examples reviewed in this paper where a gradient or a change in susceptibility can affect the magnetic field. For instance, ferromagnetic solid structures can trap the field lines and generate

a magnetic field gradient [30,36]. This idea can be extended to magnetic fluid such as ferrofluid. The advantage of using magnetic fluid is that the geometry and configuration of the magnetic structure is tunable using conventional fluidic methods. The example of isomagneto-phoresis [38] proves that this idea can work, and the use of microfluidics for tunable magnetic functions could be an exciting reasearch area in the future.

Faradaic RedOx-reactions at electrodes are interesting phenomena for supplying ions for MHD flow. With a right electrode design and chemistry, MHD flow can be utilized for designing effective micromixers. Coupling an external magnetic field into a lab-on-a-chip device not only allows magnetic manipulation but also other microfluidic functions such as pumping and mixing.

Recent works on the manipulation of contact angle of a sessile droplet using an external magnetic field indicate another trend in micro magnetofluidics: magnetowetting. There are two main strategies for magnetowetting: the manipulation of force balance at the contact line using magnetic liquid, field gradient and magnetic particles and the manipulation of surface wetting properties using magnetically responsive surface. Preliminary works show that both strategies could lead to magnetic control of a sessile droplet and offer an actuation alternative digital microfluidics.

There is still a niche for applications of MR fluids in microfluidics. Active control of MR fluid droplets would allow complex manipulation in a microfluidic network. Ferrofluid emulsion represents an interesting MR fluid, which has not been systematically explored. With microfluidic technology, high-quality monodispersed ferrofluid emulsion can be created. Fundamental investigations of ferrofluid emulsions could lead to novel applications in the near future.

The recent development of magnetic micro swimmers points to another exciting topic of micro magnetofluidics. Due to its wireless nature, magnetic field is an attractive solution for the actuation of "smart" particles. The induced magnetic force can not only be used for propulsion but also for motion control if the particle is driven by other concepts. These magnetic micro swimmers could have potential applications in micro surgery and drug delivery. Another exciting idea is the use of a large number of these magnetic micro swimmers in a droplet to gain macroscopic control over the droplet. Thus, droplet-based micro magnetofluidics can work with any liquid suitable for practical lab-on-a-chip applications.

References

1. Adams, J.D., Kim, U., Soh, H.T.: Multitarget magnetic activated cell sorter. *Proceedings of the National Academy of Sciences of the United States of America* **105**(47), 18,165–18,170 (2008)
2. Afshar, R., Moser, Y., Lehnert, T., Gijs, M.A.M.: Three-dimensional magnetic focusing of superparamagnetic beads for on-chip agglutination assays. *Analytical Chemistry* **83**(3), 1022–1029 (2011)
3. Ahn, J.J., Oh, J., Choi, B.: A novel type of a microfluidic system using ferrofluids for an application of μ -tas. *Microsystem Technologies* **10**(8-9), 622–627 (2004)
4. Ando, B., Ascia, A., Baglio, S., Beninato, A.: The "one drop" ferrofluidic pump with analog control. *Sensors and Actuators, A: Physical* **156**(1), 251–256 (2009)
5. Ando, B., Ascia, A., Baglio, S., Pitrone, N.: Ferrofluidic pumps: A valuable implementation without moving parts. *IEEE Transactions on Instrumentation and Measurement* **58**(9), 3232–3237 (2009)
6. Aussillous, P., Quéré, D.: Liquid marbles. *Nature* **411**(6840), 924–927 (2001)
7. Berim, G.O., Ruckenstein, E.: Nanodrop of an ising magnetic fluid on a solid surface. *Langmuir* **27**(14), 8753–8760 (2011)
8. Beyzavi, A., Nguyen, N.T.: One-dimensional actuation of a ferrofluid droplet by planar microcoils. *Journal of Physics D: Applied Physics* **42**(1), 015,004 (2009)
9. Beyzavi, A., Nguyen, N.T.: Programmable two-dimensional actuation of ferrofluid droplet using planar microcoils. *Journal of Micromechanics and Microengineering* **20**(1), 015,018 (2010)
10. Bormashenko, E., Pogreb, R., Bormashenko, Y., Musin, A., Stein, T.: New investigations on ferrofluidics: Ferrofluidic marbles and magnetic-field-driven drops on superhydrophobic surfaces. *Langmuir* **24**(21), 12,119–12,122 (2008)
11. Burdick, J., Laocharoensuk, R., Wheat, P.M., Posner, J.D., Wang, J.: Synthetic nanomotors in microchannel networks: Directional microchip motion and controlled manipulation of cargo. *Journal of the American Chemical Society* **130**(26), 8164–8165 (2008)
12. Chen, C., Cheng, Z.: An experimental study on rosenweig instability of a ferrofluid droplet. *Physics of Fluids* **20**(5) (2008)
13. Chen, C.Y., Chen, C., Lee, W.H.: Experiments on breakups of a magnetic fluid drop through a micro-orifice. *Journal of Magnetism and Magnetic Materials* **321**(20), 3520–3525 (2009)
14. Chen, C.Y., Wu, S.Y., Miranda, J.A.: Fingering patterns in the lifting flow of a confined miscible ferrofluid. *Physical Review E - Statistical, Nonlinear, and Soft Matter Physics* **75**(3), 036,310 (2007)
15. Choi, J.W., Liakopoulos, T.M., Ahn, C.H.: An on-chip magnetic bead separator using spiral electromagnets with semi-encapsulated permalloy. *Biosensors and Bioelectronics* **16**(6), 409–416 (2001)
16. Cowley, M.D., Rosensweig, R.E.: The interfacial instability of magnetic fluid. *Journal of Fluid Mechanics* **30**(671-688) (1967)
17. Davidson, P.A.: *An introduction to magnetohydrodynamics*. Cambridge University Press (2011)
18. Deng, T., Whitesides, G.M., Radhakrishnan, M., Zabow, G., Prentiss, M.: Manipulation of magnetic microbeads in suspension using micromagnetic systems fabricated with soft lithography. *Applied Physics Letters* **78**(12), 1775–1777 (2001)

19. Derec, C., Wilhelm, C., Servais, J., Bacri, J.: Local control of magnetic objects in microfluidic channels. *Microfluidics and Nanofluidics* **8**(1), 123–130 (2010)
20. Doyle, P.S., Bibette, J., Bancaud, A., Viovy, J.: Self-assembled magnetic matrices for dna separation chips. *Science* **295**(5563), 2237 (2002)
21. Dreyfus, R., Baudry, J., Roper, M.L., Fermigier, M., Stone, H.A., Bibette, J.: Microscopic artificial swimmers. *Nature* **437**(7060), 862–865 (2005)
22. Eijkel, J.C.T., Dalton, C., Hayden, C.J., Burt, J.P.H., Manz, A.: A circular ac magnetohydrodynamic micropump for chromatographic applications. *Sensors and Actuators, B: Chemical* **92**(1-2), 215–221 (2003)
23. Fischer, P., Ghosh, A.: Magnetically actuated propulsion at low reynolds numbers: Towards nanoscale control. *Nanoscale* **3**(2), 557–563 (2011)
24. Friedman, G., Yellen, B.: Magnetic separation, manipulation and assembly of solid phase in fluids. *Current Opinion in Colloid and Interface Science* **10**(3-4), 158–166 (2005)
25. Ganguly, R., Puri, I.K.: *Microfluidic transport in magnetic mems and biomems*. Wiley Interdisciplinary Reviews: Nanomedicine and Nanobiotechnology **2**(4), 382–399 (2010)
26. Garstecki, P., Tierno, P., Weibel, D.B., Sagus, F., Whitesides, G.M.: Propulsion of flexible polymer structures in a rotating magnetic field. *Journal of Physics Condensed Matter* **21**(20) (2009)
27. Ghost, A., Fischer, P.: Controlled propulsion of artificial magnetic nanostructured propellers. *Nano Letters* **9**(6), 2243–2245 (2009)
28. Gijs, M.A.M.: Magnetic bead handling on-chip: New opportunities for analytical applications. *Microfluidics and Nanofluidics* **1**(1), 22–40 (2004)
29. Gijs, M.A.M., Lacharme, F., Lehmann, U.: Microfluidic applications of magnetic particles for biological analysis and catalysis. *Chemical reviews* **110**(3), 1518–1563 (2010)
30. Han, K., Frazier, A.B.: Paramagnetic capture mode magnetophoretic microseparator for high efficiency blood cell separations. *Lab on a Chip - Miniaturisation for Chemistry and Biology* **6**(2), 265–273 (2006)
31. Hartshorne, H., Backhouse, C.J., Lee, W.E.: Ferrofluid-based microchip pump and valve. *Sensors and Actuators, B: Chemical* **99**(2-3), 592–600 (2004). URL www.scopus.com. Cited By (since 1996): 63
32. Hatch, A., Kamholz, A.E., Holman, G., Yager, P., Bhinger, K.F.: A ferrofluidic magnetic micropump. *Journal of Microelectromechanical Systems* **10**(2), 215–221 (2001)
33. Homsy, A., Linder, V., Lucklum, F., de Rooij, N.F.: Magnetohydrodynamic pumping in nuclear magnetic resonance environments. *Sensors and Actuators, B: Chemical* **123**(1), 636–646 (2007)
34. Jang, J., Lee, S.S.: Theoretical and experimental study of mhd (magnetohydrodynamic) micropump. *Sensors and Actuators, A: Physical* **80**(1), 84–89 (2000)
35. Joung, J., Shen, J., Grodzinski, P.: Micropumps based on alternating high-gradient magnetic fields. *IEEE Transactions on Magnetics* **36**(4 PART 2), 2012–2014 (2000)
36. Jung, Y., Choi, Y., Han, K., Frazier, A.B.: Six-stage cascade paramagnetic mode magnetophoretic separation system for human blood samples. *Biomedical Microdevices* **12**(4), 637–645 (2010)
37. Kang, H., Choi, B.: Development of the mhd micropump with mixing function. *Sensors and Actuators, A: Physical* **165**(2), 439–445 (2011)
38. Kang, J.H., Choi, S., Lee, W., Park, J.: Isomagneto-phoresis to discriminate subtle difference in magnetic susceptibility. *Journal of the American Chemical Society* **130**(2), 396–397 (2008)
39. Kang, J.H., Park, J.: Magnetophoretic continuous purification of single-walled carbon nanotubes from catalytic impurities in a microfluidic device. *Small* **3**(10), 1784–1791 (2007)
40. Kline, T.R., Paxton, W.F., Mallouk, T.E., Sen, A.: Catalytic nanomotors: Remote-controlled autonomous movement of striped metallic nanorods. *Angewandte Chemie - International Edition* **44**(5), 744–746 (2005)
41. Kong, T.F., Huan Shin, E.H.S., Sugiarto, H.S., Liew, H.F., Wang, X., Lew, W.S., Nguyen, N.T., Chen, Y.: An efficient microfluidic sorter: Implementation of double meandering micro striplines for magnetic particles switching. *Microfluidics and Nanofluidics* **10**(5), 1069–1078 (2011)
42. Krishnan, J.N., Kim, C., Park, H.J., Kang, J.Y., Kim, T.S., Kim, S.K.: Rapid microfluidic separation of magnetic beads through dielectrophoresis and magnetophoresis. *Electrophoresis* **30**(9), 1457–1463 (2009)
43. Lee, H., Purdon, A.M., Westervelt, R.M.: Manipulation of biological cells using a microelectromagnet matrix. *Applied Physics Letters* **85**(6), 1063–1065 (2004)
44. Lemoff, A.V., Lee, A.P.: Ac magnetohydrodynamic micropump. *Sensors and Actuators, B: Chemical* **63**(3), 178–185 (2000)
45. Lemoff, A.V., Lee, A.P.: An ac magnetohydrodynamic microfluidic switch for micro total analysis systems. *Biomedical Microdevices* **5**(1), 55–60 (2003)
46. Leventis, N., Gao, X.: Magnetohydrodynamic electrochemistry in the field of nd-fe-b magnets. theory, experiment, and application in self-powered flow delivery systems. *Analytical Chemistry* **73**(16), 3981–3992 (2001)
47. Li, Q., Lian, W., Sun, H., Xuan, Y.: Investigation on operational characteristics of a miniature automatic cooling device. *International Journal of Heat and Mass Transfer* **51**(21-22), 5033–5039 (2008)
48. Lian, W., Xuan, Y., Li, Q.: Design method of automatic energy transport devices based on the thermomagnetic effect of magnetic fluids. *International Journal of Heat and Mass Transfer* **52**(23-24), 5451–5458 (2009)
49. Liu, J., Lawrence, E.M., Wu, A., Ivey, M.L., Flores, G.A., Javier, K., Bibette, J., Richard, J.: Field-induced structures in ferrofluid emulsions. *Physical Review Letters* **74**(14), 2828–2831 (1995)
50. Liu, J., Tan, S.H., Yap, Y.F., Ng, M.Y., Nguyen, N.T.: Numerical and experimental investigations of the formation process of ferrofluid droplets. *Microfluidics and Nanofluidics* **11**(2), 177–187 (2011)
51. Liu, J., Yap, Y.F., Ng, M.Y., Nguyen, N.T.: Numerical study of the formation process of ferrofluid droplets. *Physics of Fluids* **23**(7), 072,008 (2011)
52. Love, L.J., Jansen, J.F., McKnight, T.E., Roh, Y., Phelps, T.J.: A magnetocaloric pump for microfluidic applications. *IEEE Transactions on Nanobioscience* **3**(2), 101–110 (2004)
53. Mao, L., Elborai, S., He X. amd Zahn, M., Koser, H.: Direct observation of closed-loop ferrohydrodynamic pumping under traveling magnetic fields. *Physical Review B* **84**(10), 104,431 (2011)
54. Mao, L., Koser, H.: Towards ferrofluidics for μ -tas and lab on-a-chip applications. *Nanotechnology* **17**(4), S34–S47 (2006)
55. Murshed, S.M.S., Tan, S.H., Nguyen N. T. abd Wong, T.N., Yobas, L.: Microdroplet formation of water and

- nanofluids in heat-induced microfluidic t-junction. *Micro and Nanosystems* **6**(6), 253–259 (2009)
56. Nguyen, B., Kassegne, S.K.: High-current density dc magnetohydrodynamics micropump with bubble isolation and release system. *Microfluidics and Nanofluidics* **5**(3), 383–393 (2008)
 57. Nguyen, N., Ting, T., Yap, Y., Wong, T., Chai, J.C., Ong, W., Zhou, J., Tan, S., Yobas, L.: Thermally mediated droplet formation in microchannels. *Applied Physics Letters* **91**(8) (2007). URL www.scopus.com. Cited By (since 1996): 23
 58. Nguyen, N.T., Chai, M.F.: A stepper micropump for ferrofluid driven microfluidic systems. *Micro and Nanosystems* **1**(1), 17–21 (2009)
 59. Nguyen, N.T., Ng, K.M., Huang, X.: Manipulation of ferrofluid droplets using planar coils. *Applied Physics Letters* **89**(5), 052,509 (2006)
 60. Nguyen, N.T., Zhu, G.P., Chua, Y., Phan, V.N., Tan, S.H.: Magnetowetting and sliding motion of a sessile ferrofluid droplet in the presence of a permanent magnet. *Langmuir* **26**(15), 12,553–12,559 (2010)
 61. Niu, X., Zhang, M., Wu, J., Wen, W., Sheng, P.: Generation and manipulation of "smart" droplets. *Soft Matter* **5**(3), 576–581 (2009)
 62. Pal, S., Datta, A., Sen, S., Mukhopdhyay, A., Bandopadhyay, K., Ganguly, R.: Characterization of a ferrofluid-based thermomagnetic pump for microfluidic applications. *Journal of Magnetism and Magnetic Materials* (2011). Article in Press
 63. Pamme, N.: Magnetism and microfluidics. *Lab on a Chip - Miniaturisation for Chemistry and Biology* **6**(1), 24–38 (2006)
 64. Pamme, N., Eijkel, J.C.T., Manz, A.: On-chip free-flow magnetophoresis: Separation and detection of mixtures of magnetic particles in continuous flow. *Journal of Magnetism and Magnetic Materials* **307**(2), 237–244 (2006)
 65. Pamme, N., Manz, A.: On-chip free-flow magnetophoresis: Continuous flow separation of magnetic particles and agglomerates. *Analytical Chemistry* **76**(24), 7250–7256 (2004)
 66. Plouffe, B.D., Lewis, L.H., Murthy, S.K.: Computational design optimization for microfluidic magnetophoresis. *Biomicrofluidics* **5**(1), 013,413 (2011)
 67. Probst, R., Lin, J., Komae, A., Nacev, A., Cummins, Z., Shapiro, B.: Planar steering of a single ferrofluid drop by optimal minimum power dynamic feedback control of four electromagnets at a distance. *Journal of Magnetism and Magnetic Materials* **323**(7) (2011)
 68. Qian, S.Z., Bau, H.H.: Magneto-hydrodynamics based microfluidics. *Mechanics Research Communications* **36**(1), 382–399 (2009)
 69. Rhodes, S., Perez, J., Elborai, S., Lee, S., Zahn, M.: Ferrofluid spiral formations and continuous-to-discrete phase transitions under simultaneously applied dc axial and ac in-plane rotating magnetic fields. *Journal of Magnetism and Magnetic Materials* **289**, 353–355 (2005)
 70. Rong, R., Choi, J.W., Ahn, C.H.: An on-chip magnetic bead separator for biocell sorting. *Journal of Micromechanics and Microengineering* **16**(12), 2783–2790 (2006)
 71. Rosensweig, R.E.: *Ferrohydrodynamics*. Dover Publications (1997)
 72. Siegel, A.C., Bruzewicz, D.A., Weibel, D.B., Whitesides, G.M.: Microsolidics: Fabrication of three-dimensional metallic microstructures in poly(dimethylsiloxane). *Advanced Materials* **19**(5), 727–733 (2007)
 73. Siegel, A.C., Shevkoplyas, S.S., Weibel, D.B., Bruzewicz, D.A., Martinez, A.W., Whitesides, G.M.: Cofabrication of electromagnets and microfluidic systems in poly(dimethylsiloxane). *Angewandte Chemie - International Edition* **45**(41), 6877–6882 (2006)
 74. Smistrup, K., Kjeldsen, B.G., Reimers, J.L., Dufva, M., Petersen, J., Hansen, M.F.: On-chip magnetic bead microarray using hydrodynamic focusing in a passive magnetic separator. *Lab on a Chip - Miniaturisation for Chemistry and Biology* **5**(11), 1315–1319 (2005)
 75. Song, S.H., Lee, H.L., Min, Y.H., Jung, H.I.: Electromagnetic microfluidic cell labeling device using on-chip microelectromagnet and multi-layered channels. *Sensors and Actuators, B: Chemical* **141**(1), 210–216 (2009)
 76. Sun, Y., Kwok, Y.C., Foo-Peng Lee, P., Nguyen, N.T.: Rapid amplification of genetically modified organisms using a circular ferrofluid-driven pcr microchip. *Analytical and Bioanalytical Chemistry* **394**(5), 1505–1508 (2009)
 77. Sun, Y., Kwok, Y.C., Nguyen, N.T.: A circular ferrofluid driven microchip for rapid polymerase chain reaction. *Lab on a Chip - Miniaturisation for Chemistry and Biology* **7**(8), 1012–1017 (2007)
 78. Sun, Y., Nguyen, N.T., Yien, C.K.: High-throughput polymerase chain reaction in parallel circular loops using magnetic actuation. *Analytical Chemistry* **80**(15), 6127–6130 (2008)
 79. Suwa, M., Watarai, H.: Magnetoanalysis of micro/nanoparticles: A review. *Analytica Chimica Acta* **690**(2), 137–147 (2011)
 80. Tan, S.H., Nguyen, N.T.: Generation and manipulation of monodispersed ferrofluid emulsion: the effect of a uniform magnetic field in flow-focusing and t-junction configurations. *Physical Review E* **84**(3), 036,317 (2011)
 81. Tan, S.H., Nguyen, N.T., Yobas, L., Kang, T.G.: Formation and manipulation of ferrofluid droplets at a microfluidic t-junction. *Journal of Micromechanics and Microengineering* **20**(4), 045,004 (2010)
 82. Tierno, P., Golestanian, R., Pagonabarraga, I., Sagus, F.: Controlled swimming in confined fluids of magnetically actuated colloidal rotors. *Physical Review Letters* **101**(21) (2008)
 83. Tierno, P., Golestanian, R., Pagonabarraga, I., Sagus, F.: Magnetically actuated colloidal microswimmers. *Journal of Physical Chemistry B* **112**(51), 16,525–16,528 (2008)
 84. Wang, L., Zhang, M., Li, J., Gong, X., Wen, W.: Logic control of microfluidics with smart colloid. *Lab on a Chip - Miniaturisation for Chemistry and Biology* **10**(21), 2869–2874 (2010)
 85. Watarai, H., Namba, M.: Magnetophoretic behavior of single polystyrene particles in aqueous manganese(ii) chloride. *Analytical Sciences* **17**(10), 1233–1236 (2001)
 86. Weddemann, A., Albon, C., Auge, A., Wittbracht, F., Hedwig, P., Akemeier, D., Rott, K., Meiner, D., Jutzi, P., Httten, A.: How to design magneto-based total analysis systems for biomedical applications. *Biosensors and Bioelectronics* **26**(4), 1152–1163 (2010)
 87. West, J., Gleeson, J.P., Alderman, J., Collins, J.K., Berney, H.: Structuring laminar flows using annular magnetohydrodynamic actuation. *Sensors and Actuators, B: Chemical* **96**(1-2), 190–199 (2003)
 88. Weston, M.C., Gerner, M.D., Fritsch, I.: Magnetic fields for fluid motion. *Analytical Chemistry* **82**(9), 3411–3418 (2010)
 89. Wirix-Speetjens, R., De Boeck, J.: On-chip magnetic particle transport by alternating magnetic field gradients. *IEEE Transactions on Magnetics* **40**(4 I), 1944–1946 (2004)

90. Xuan, Y., Lian, W.: Electronic cooling using an automatic energy transport device based on thermomagnetic effect. *Applied Thermal Engineering* **31**(8-9), 1487–1494 (2011)
91. Xue, Y., Wang, H., Zhao, Y., Dai, L., Feng, L., Wang, X., Lin, T.: Magnetic liquid marbles: A "precise" miniature reactor. *Advanced Materials* **22**(43), 1–5 (2010)
92. Yamahata, C., Chastellain, M., Parashar, V.K., Petri, A., Hofmann, H., Gijs, M.A.M.: Plastic micropump with ferrofluidic actuation. *Journal of Microelectromechanical Systems* **14**(1), 96–102 (2005)
93. Zhang, L., Abbott, J.J., Dong, L., Peyer, K.E., Kratochvil, B.E., Zhang, H., Bergeles, C., Nelson, B.J.: Characterizing the swimming properties of artificial bacterial flagella. *Nano Letters* **9**(10), 3663–3667 (2009)
94. Zhang, M., Gong, X., Wen, W.: Manipulation of microfluidic droplets by electrorheological fluid. *Electrophoresis* **30**(18), 3116–3123 (2009)
95. Zhao, Y., Fang, J., Wang, H., Wang, X., Lin, T.: Magnetic liquid marbles: Manipulation of liquid droplets using highly hydrophobic Fe_3O_4 nanoparticles. *Advanced Materials* **22**(6), 707–710 (2010)
96. Zhong, J.H., Yi, M.Q., Bau, H.H.: Magneto hydrodynamic (mhd) pump fabricated with ceramic tapes. *Sensors and Actuators, A: Physical* **96**(1), 59–66 (2002)
97. Zhou, Q., Ristenpart, W.D., Stroeve, P.: Magnetically induced decrease in droplet contact angle on nanostructured surfaces. *Langmuir* **27**(19), 11,747–11,751 (2011)